

GLUCOSE DIFFUSION IN PANCREATIC ISLETS OF LANGERHANS *

RICHARD BERTRAM[†] AND MARK PERNAROWSKI[‡]

[†] School of Science, Pennsylvania State University, Erie, PA 16563

[‡] Department of Mathematical Sciences, Montana State University, Bozeman, MT 59717

Abstract. We investigate the time required for glucose to diffuse through an isolated pancreatic islet of Langerhans and reach an equilibrium. This question is relevant in the context of *in vitro* electrophysiological studies of the response of an islet to step changes in the bath glucose concentration. Islet cells are electrically coupled by gap junctions, so nonuniformities in islet glucose concentration may be reflected in the activity of cells on the islet periphery, where electrical recordings are made. Using a mathematical model of hindered glucose diffusion, we investigate the effects of the islet porosity and the permeability of a surrounding layer of acinar cells. A major factor in the determination of the equilibrium time is the transport of glucose into islet β -cells, which removes glucose from the interstitial spaces where diffusion occurs. This transport is incorporated using a model of the GLUT-2 glucose transporter. We find that several minutes are required for the islet to equilibrate to a 10 mM change in bath glucose, a typical protocol in islet experiments. It is therefore likely that in electrophysiological islet experiments the glucose distribution is nonuniform for several minutes following a step change in bath glucose. The delay in glucose penetration to the inner portions of the islet may be a major contributing factor to the one to two minute delay in islet electrical activity typically observed following bath application of a stimulatory concentration of glucose.

Running title: Glucose Diffusion in Pancreatic Islets

Keywords: β -cells, mathematical modeling, islets of Langerhans

*Address reprint requests to Dr. Richard Bertram, School of Science, Pennsylvania State University, Erie, PA 16563. Tel.: 814-898-6090, Fax: 814-898-6213, E-mail: bertram@euler.bd.psu.edu.

INTRODUCTION

The endocrine pancreas plays a key role in blood glucose homeostasis. It is here that insulin is secreted into the blood stream in response to an elevation in blood glucose, initiating a cascade of events leading to the uptake of glucose by muscle and adipose tissue. The secretory cells responsible for the release of insulin, pancreatic β -cells, are clustered into micro-organs called islets of Langerhans. These are roughly spherical structures of radius 50–250 μm in which the β -cells and other secretory cells are densely packed. Within the pancreas there are on the order of 10^6 islets, and within each islet there are 10^3 – 10^4 β -cells and 100–200 secretory cells of other types.

Pancreatic β -cells are electrically excitable, and *in vitro* studies of isolated islets have shown that β -cells depolarize when the glucose concentration in the bath solution is increased (Dean and Mathews, 1970). This depolarization initiates periodic bursts of action potentials which evoke the secretion of insulin (Scott et al., 1981; Atwater et al., 1989). Periodic bursting behavior has also been observed *in vivo*, with a burst period (tens of seconds) similar to that observed *in vitro* (Sánchez-Andrés et al., 1995).

The electrical nature of the insulin secretion process has prompted numerous electrophysiological studies of isolated β -cells and β -cells in intact islets. The latter studies are necessary since isolated cells either do not burst, or burst with an abnormally long period of several minutes (Smith et al., 1990; Larsson et al., 1996). In islet studies (Atwater et al., 1989), the islet is secured to the bottom of a perfusion chamber through which perfusion solution is continuously exchanged. Secretagogues such as glucose are introduced into the solution in a separate mixing chamber and enter the perfusion chamber through an inflow tube. Because glucose is the primary endogenous modulator of β -cell electrical activity, a common experimental protocol is to make a step change in the bath glucose concentration and study the response of the islet in the presence or absence of other modulators. It is therefore important to establish bounds on the time required for glucose to diffuse through the islet and reach a new equilibrium distribution.

In the present study we perform a mathematical analysis of the diffusion of glucose in an isolated islet using a model islet which is assumed for simplicity to be composed solely of β -cells. Several factors hinder glucose diffusion in an islet, and we investigate the effects of each. First, glucose diffuses primarily through the narrow interstitial spaces between islet cells. We account for this by introducing an “effective” glucose diffusion rate that reflects the islet porosity. This rate is varied to determine the effect of porosity on glucose penetration into the islet. Second, the islet is surrounded by a layer of pancreatic acinar cells, which forms a diffusion barrier between the islet and the surrounding bath solution.

Since the permeability of this tissue will vary from islet to islet, we study the effects on glucose penetration of variations in the acinar layer permeability. Finally, as glucose diffuses through the islet it is transported into β -cells by GLUT-2 glucose transporters, thus removing it from the interstitial spaces where diffusion occurs. Using values for the GLUT-2 transport rate obtained experimentally (Johnson et al., 1990), we investigate the effect of GLUT-2 transporters on glucose penetration into the islet.

Our analysis indicates that if 10 mM glucose (a typical value for *in vitro* experiments) is added to a glucose-free bath, then the glucose distribution in the islet will be nonuniform for several minutes. For an islet of 200 μm diameter and with maximum or saturating values of porosity and permeability, it takes five minutes for the glucose concentration at the islet center to reach 90% of the bath concentration. The equilibration time is longer in larger islets. Removal of glucose from the interstitial solution by GLUT-2 transporters profoundly slows glucose penetration to the islet center, as less than one minute is required for 90% equilibration in the absence of GLUT-2 transport. Islet porosity and acinar layer permeability also have profound effects on glucose penetration, with the impact of one parameter depending on the value of the other and the location in the islet.

Experimental data regarding the time course of glucose penetration into an islet is very limited. However, in recent work by Bennett et al. (1996) two-photon excitation microscopy was used to measure time-dependent glucose-induced NAD(P)H autofluorescence changes in an optical section of an intact islet. This data provides an indication of the time course of the intracellular glucose concentration following a step change in bath glucose, and we compare this to the glucose time course predicted from the model. We find that the autofluorescence data can be accounted for by the model, particularly if one or two of the model parameters are appropriately modified or if some glucose diffusion between β -cells is allowed.

One feature consistently observed in *in vitro* perfusion studies is a delay of one to two minutes between the addition of glucose to a previously low-glucose or glucose-free solution, and the start of β -cell electrical activity (Atwater et al., 1989; Worley et al., 1994). This cannot be explained by the delay in glucose transport from the mixing chamber to the perfusion chamber, which is typically only a few seconds (Mears, 1996; Soria et al., 1996). One contributing factor in the delay is the time required for the metabolism of glucose within the β -cells, and for the product ATP to inactivate ATP-sensitive potassium channels and depolarize the cells (Ashcroft et al., 1984; Chow et al., 1995). Another contributing factor is the time required for glucose to diffuse from the islet periphery to the islet center, although until now no mathematical study has been

performed to determine the importance of this factor. Also, islet cells are electrically coupled by gap junctions, which tend to synchronize β -cell electrical activity (Eddlestone et al., 1984; Santos et al., 1991). Silent cells in the islet interior can therefore restrain cells on the periphery from firing, although it is not known what fraction of the cells must be activated by glucose for synchronized electrical activity to occur. Our analysis suggests that the time required for glucose penetration into the interior of the islet is a major contributing factor in the one to two minute delay in electrical activity.

The results of this study suggest that care should be taken when interpreting data recorded within a few minutes of a change in glucose concentration. A non-uniform glucose distribution may have unsuspected effects on the electrical activity of the islet and the response of the islet to chemical modulators, complicating the already difficult analysis of experimental data.

In the following sections we first describe the mathematical model for glucose diffusion in an islet, and then proceed with an analysis of the extent of glucose penetration and equilibration times, first without, and then with GLUT-2 glucose transporters. We then compare model simulations with recent NAD(P)H autofluorescence data. Parameter values used throughout are summarized in Appendix II.

THE MATHEMATICAL MODEL

To make electrical recordings of β -cells in an intact islet, the islet must first be secured within the perfusion chamber. This has been done in several ways, such as inserting pins through the surrounding acinar tissue (Atwater et al., 1989; Soria et al., 1996); inserting pins through a piece of pancreas and exposing one or more islets to the perfusion solution (Henquin et al., 1988); or securing the islet with a suction pipette (Cook and Perara, 1982). Once secured, a recording electrode is inserted into a cell on the islet periphery. The rate of solution perfusion varies, but typical values are 1 to 2 ml/min. The volume of a typical perfusion chamber is 40 to 50 μ l, so the bath solution is replaced every few seconds, assuring that the composition of the solution can be rapidly changed. The diameter of a pancreatic islet is 100–500 μ m, so islet volume is no greater than about $\frac{4}{3}\pi(0.25)^3 \approx 6.5 \times 10^{-2}$ mm³, or 6.5×10^{-2} μ l in terms of fluid volume. Hence, the islet volume is negligible compared to the volume of the bath.

When a secretagogue such as glucose is introduced into the perfusion solution it enters the islet through convection and diffusion. We make the simplifying assumption that glucose enters the islet solely through diffusion, and further assume that the bath solution is uniformly mixed. These two assumptions allow us to neglect the convection

and mixing of the perfusion solution with the secretagogue, and to focus on the diffusion of glucose into and within the islet.

When glucose penetrates the acinar layer surrounding the islet it is free to diffuse through the interstitial spaces between adjacent β -cells (Fig. 1). We treat this as a hindered diffusion process, and define a variable g_e that represents the extracellular (or interstitial) glucose concentration as a function of time and position within the islet. Spherical coordinates are used to describe position and we assume spherical symmetry in the glucose distribution. With these assumptions, the diffusion of glucose through an islet of radius a is described by

$$(1) \quad \frac{\partial g_e}{\partial t} = pD \frac{1}{r^2} \frac{\partial}{\partial r} \left(r^2 \frac{\partial g_e}{\partial r} \right) - \frac{1}{\rho} F(g_e, g_i), \quad r < a, \quad t > 0.$$

Here D is the diffusion coefficient of glucose in water and pD is the “effective” glucose diffusion coefficient within the islet. The dimensionless parameter $p \in [0, 1]$ is a measure of islet porosity and reflects a diminished random walk due to cell geometry and cell packing.

The function $F(g_e, g_i)$ in Eq. (1) represents glucose transport into the β -cells through GLUT-2 glucose transporters in the cells’ plasma membrane. The rate of uptake of glucose by these transporters depends on both the glucose concentration within the β -cells (g_i) and that in the surrounding extracellular space. We assume that transport is uniform throughout the islet, so that F is independent of r . The specific form of this transport term will be described in detail later. The parameter ρ is the volume fraction: $\rho = V_e/V_i$ where V_i is the total β -cell volume within the islet and V_e is the total volume of the extracellular space.

We assume that the acinar tissue surrounding the islet can be modeled as a passive membrane. Therefore, the chemical gradient across this tissue is the only source for the flux of glucose into the islet and an appropriate boundary condition is:

$$(2) \quad \frac{\partial g_e}{\partial r} = k(G - g_e) \quad , \quad r = a \quad , \quad k > 0,$$

where G is the glucose concentration in the perfusion solution and k is the permeability of the acinar layer. A singularity condition is applied at the islet center,

$$(3) \quad |g_e(0, t)| \leq M < \infty \quad , \quad t \geq 0.$$

Finally, unless otherwise stated, we assume that the initial glucose concentration in the islet is zero,

$$(4) \quad g_e(r, 0) = 0 \quad , \quad r \in [0, a].$$

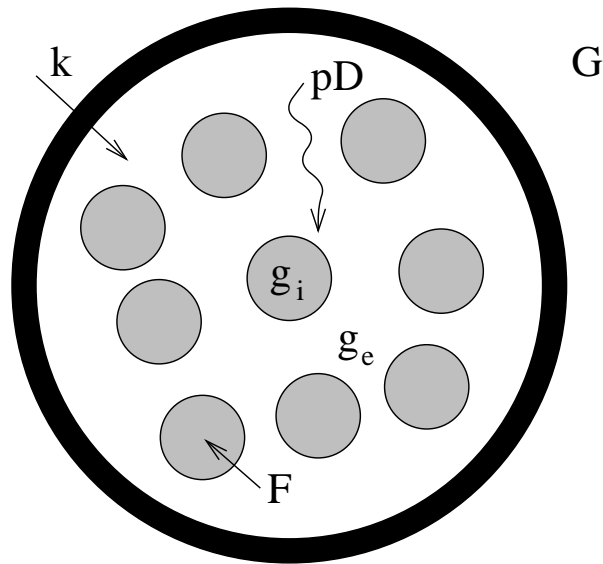


FIG. 1. Illustration of the islet model, highlighting the roles of the variables and parameters in Eqs. 1–5. The dark shell represents the acinar layer, the shaded circles represent β -cells, and the space between represents the interstitial region through which glucose diffuses. (The proportion of interstitial space to β -cell space is exaggerated.) The space outside of the shell represents the region occupied by well-mixed perfusion solution. Arrows represent the flow of glucose.

As with the interstitial glucose concentration, we treat the glucose concentration within the β -cells as a continuous variable that depends on both time and location within the islet. Although there is some evidence that sugars can pass through gap junctions (Rieske et al., 1975), we assume that glucose diffusion through gap junctions does not occur. (This assumption is relaxed later.) Thus, the differential equation describing glucose concentration within the β -cells (g_i) contains no spatial derivatives:

$$(5) \quad \frac{\partial g_i}{\partial t} = F(g_e, g_i).$$

Unless otherwise stated, the initial β -cell glucose concentration is also taken to be zero,

$$(6) \quad g_i(r, 0) = 0 \quad , \quad r \in [0, a].$$

Metabolism of glucose by the β -cells is not included in Eq. 5 since cell culture studies have shown that the glucose concentration inside a β -cell rapidly approaches an equilibrium that is only slightly lower than the concentration outside the cell (Whitesell et al., 1991).

RESULTS

Glucose Diffusion Without Transport

We first analyze the diffusion of glucose in the absence of glucose transport, $F(g_e, g_i) = 0$,

focusing on the effects on equilibration times of different islet porosities (through the parameter p) and acinar layer permeabilities (through k). With $F(g_e, g_i) = 0$ the differential equations Eq. 1 and Eq. 5 are uncoupled, simplifying the analysis of Eqs. 1–4.

We begin by deriving an approximate expression for the glucose diffusion time, making use of the linearity of the uncoupled differential equation Eq. 1. The derivation, based on the method of separation of variables, requires that we first homogenize the boundary conditions with the introduction of a new variable $c = G - g_e$. This variable transformation emphasizes the point that in the absence of glucose transport the equilibration time does not depend on the initial values of g_e and G , only the difference between them. In terms of the new variable, Eqs. 1–4 become

$$(7) \quad \frac{\partial c}{\partial t} = pD \frac{1}{r^2} \frac{\partial}{\partial r} \left(r^2 \frac{\partial c}{\partial r} \right), \quad r < a, \quad t > 0 \quad ,$$

$$(8) \quad \frac{\partial c}{\partial r} + kc = 0 \quad , \quad r = a \quad , \quad t > 0 \quad ,$$

$$(9) \quad |c(0, t)| \leq M < \infty \quad , \quad t \geq 0 \quad ,$$

$$(10) \quad c(r, 0) = G.$$

The calculations leading to the series solution of Eqs. 7–10 are detailed in Appendix I. The results of these calculations yield the solution

$$(11) \quad c(r, t) = G \sum_{n=1}^{\infty} a_n \exp(-\lambda_n^2 pDt) \frac{\sin(\lambda_n r)}{\sqrt{\lambda_n r}} \quad ,$$

where the eigenvalues λ_n ($0 < \lambda_1 < \lambda_2 < \dots$) satisfy the eigenvalue equation

$$(12) \quad (ka - 1) \tan \mu_n + \mu_n = 0 \quad , \quad \mu_n = \lambda_n a \quad .$$

Since the decay of the first Fourier mode is rate limiting, the rate at which interstitial glucose equilibrates to the external concentration G (or equivalently the rate at which c approaches zero) depends primarily on the value of the dominant eigenvalue λ_1 . In subsequent calculations, we compute this dominant eigenvalue for each of several values of k by finding the equilibria $\mu_1 = \lambda_1 a$ of the differential equation

$$(13) \quad \frac{d\mu}{dt} = (ka - 1) \tan \mu + \mu \quad ,$$

in the interval $(0, \pi)$. These computations were done numerically using the bifurcation software package AUTO (Doedel, 1981), with k as the bifurcation parameter. Such a calculation is equivalent to finding the roots of Eq. 12.

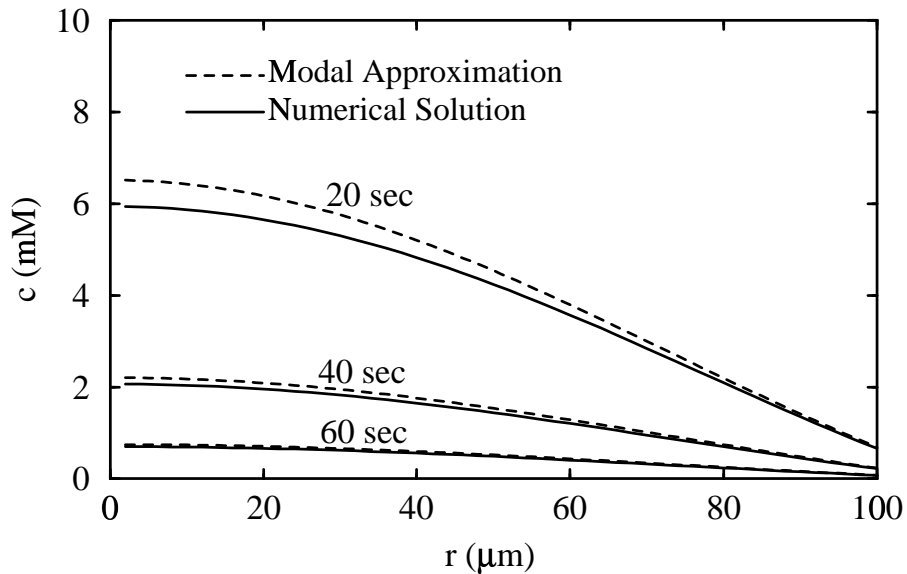


FIG. 2. Comparison of the numerical solution to Eqs. 7–10 and the dominant mode approximation Eq. 14 at several different times following the simulated bath application of 10 mM glucose ($G = 10$ mM). Computations were performed with permeability $k = 0.1 \mu\text{m}^{-1}$, porosity $p = 0.1$, and islet radius $a = 100 \mu\text{m}$.

The dominant mode approximation to the series solution Eq. 11 is

$$(14) \quad c(r, t) \simeq c_1(r, t) = Ga_1 \exp(-\lambda_1^2 p D t) \frac{\sin(\lambda_1 r)}{\sqrt{\lambda_1 r}} .$$

To verify the accuracy of this approximation we compare it with the numerical solution of Eqs. 7–10 at several different times following the simulated bath application of 10 mM glucose (Fig. 2). (The details of the numerical method are described in the next section.) The accuracy of the modal approximation appears to be quite good, improving with time so that after one minute the modal approximation and numerical solution are practically indistinguishable.

One measure of the glucose equilibration time is the time T_f required for glucose concentration at the islet center to reach some fraction f of that in the surrounding bath solution:

$$(15) \quad g_e(0, T_f) = fG .$$

Since $c = G - g_e$, this definition is equivalent to $c(0, T_f) = (1 - f)G$. Using the modal approximation for $c(r, T_f)$ and taking the limit as $r \rightarrow 0^+$,

$$(16) \quad (1 - f)G = Ga_1 \sqrt{\lambda_1} \exp(-\lambda_1^2 p D T_f) .$$

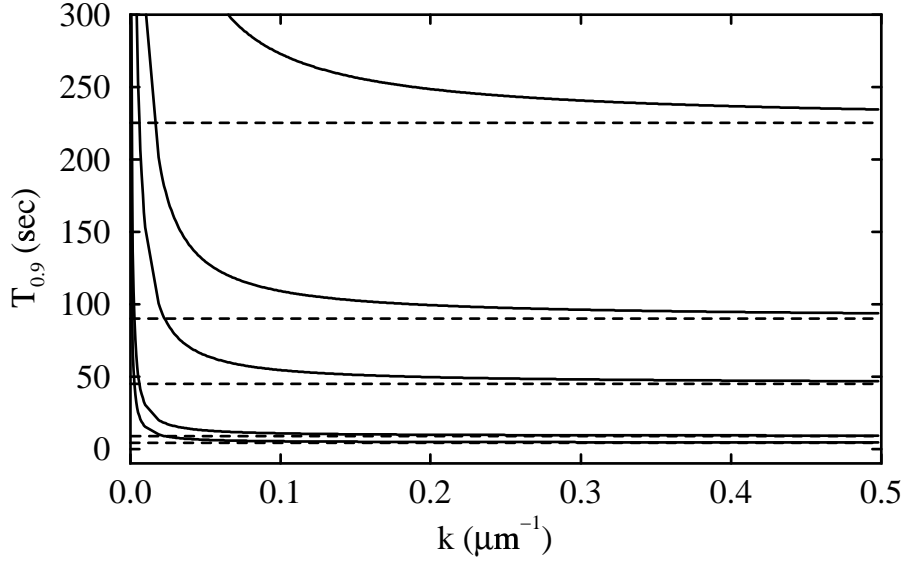


FIG. 3. Time $T_{0.9}$ required for glucose concentration at the center of the islet to attain 90% ($f = 0.9$) of the equilibrium value G in the absence of GLUT-2 transport. Values of $T_{0.9}$ are plotted for $p = 0.02, 0.05, 0.1, 0.5$ and 1 (from top to bottom). Dashed horizontal lines indicate the large ka approximation of $T_{0.9}$ given in Eq. 18.

Solving this for T_f yields the characteristic diffusion time

$$(17) \quad T_f = \frac{1}{\lambda_1^2 p D} \ln \left(\frac{a_1 \sqrt{\lambda_1}}{1-f} \right) .$$

It is evident in Eq. 17 that the diffusion time is inversely proportional to the islet porosity p . However, the dependence of T_f on the islet radius a and the acinar layer permeability k are not immediately evident. The dependence on a becomes clear for ka large, in which case $\mu_1 \approx \pi$, so $\lambda_1 \approx \pi/a$. Thus, the Fourier coefficient $a_1 \approx 2\sqrt{a/\pi}$ (see Appendix I) and

$$(18) \quad T_f \approx \frac{a^2}{\pi^2 p D} \ln \left(\frac{2}{1-f} \right) , \quad ka \text{ large.}$$

Hence, for ka large the characteristic diffusion time is proportional to the square of the islet radius.

The dependence of T_f on k is illustrated in Fig. 3, where $T_{0.9}$ (i.e., the time at which $g_e = 0.9G$ at the islet center) is plotted versus k for several values of porosity p . As expected, T_f is a decreasing function of the acinar tissue permeability. We see in Fig. 3,

however, that the influence of permeability is different for different porosities, the influence being greatest when porosity is low. In this case, changes in k have a significant impact on $T_{0.9}$ for all values of k . In contrast, if porosity is high then the characteristic diffusion time is insensitive to changes in k for $k > 0.1 \mu\text{m}^{-1}$. Fig. 3 also shows that for all but the lowest value of porosity, Eq. 18 provides a good approximation to the characteristic diffusion time for ka large.

The Effect of GLUT-2 Glucose Transporters

Glucose molecules are transported across the β -cell membrane by a process of facilitated diffusion. Although several different glucose transporters have been identified in a number of cell types (Unger, 1991), studies have shown that glucose transport in β -cells is due primarily to the GLUT-2 transporter (Johnson et al., 1990; Heimberg et al., 1995). In this section, we incorporate a model of GLUT-2 glucose transport into the g_e and g_i equations (Eqs. 1 and 5). This allows us to investigate the impact of GLUT-2 transport on glucose penetration, and allows us to monitor the glucose concentration within the β -cells as well as in the interstitial spaces.

A 4-state kinetic model of the GLUT-2 transporter has been developed by Maki and Keizer (1995). In this model, there is a glucose-free state with the transporter facing into the cell; a glucose-free state with the transporter facing out of the cell; and two similar glucose-bound states. In the development of the model it was assumed that binding of the transporter is in rapid equilibrium and that all rate constants for crossing the membrane are equal. In terms of the variables g_e and g_i , the glucose flux into the cell, F , is

$$(19) \quad F(g_e, g_i) = V_{max} \frac{(g_e - g_i)K_m}{(K_m + g_e)(K_m + g_i)}$$

where V_{max} and K_m are the maximum transport rate and transporter dissociation constant, respectively. Values for these parameters have been determined in studies of glucose uptake in dispersed rat islet cells: $V_{max} = 32$ mmole/min per liter of islet space or 0.53 mM/sec, and $K_m = 17$ mM (Johnson et al., 1990).

The complete model of glucose diffusion with GLUT-2 transport is obtained by combining Eq. 19 with Eqs. 1–5. The flux term Eq. 19 is scaled by the volume fraction $\rho = V_e/V_i$ in Eq. 1 to reflect the different volumes of the extracellular and intracellular regions. Electron micrograph studies indicate that the extracellular volume is 1–2% of the total islet volume (Bonner-Weir, 1988), so we use $\rho = 0.02$ for the volume fraction.

With the introduction of the transport term, the g_e and g_i equations are coupled and nonlinear. We integrated these equations numerically with the software package XTC

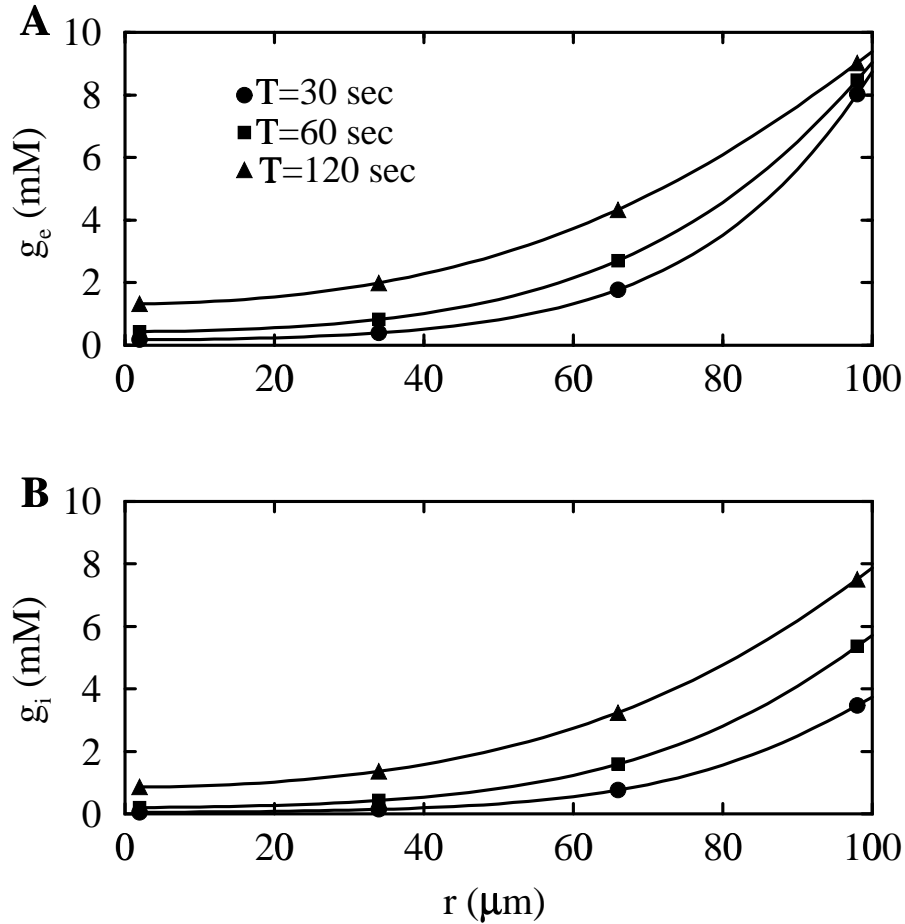


FIG. 4. Glucose distribution in the islet at three different times following the simulated bath application of 10 mM glucose ($G = 10$ mM). **A.** Glucose concentration in the interstitial spaces (g_e). **B.** Glucose concentration within the β -cells (g_i). Initially $g_e = g_i = 0$ throughout the islet. Islet porosity and the acinar layer permeability are $p = 0.3$ and $k = 0.3 \mu\text{m}^{-1}$, respectively.

(Ermentrout, 1995), using an implicit backwards Euler method with $\Delta t = 0.1$ sec and $\Delta r = 2 \mu\text{m}$. Unless stated otherwise, the computations use an islet radius of $a = 100 \mu\text{m}$. To eliminate the removable singularity at the islet center we applied the variable transformations $\zeta_e = g_e r$ and $\zeta_i = g_i r$. All results are reported in terms of the original variables g_e and g_i .

Figure 4 shows the spatial distribution of g_e and g_i at different times after the simulated bath application of 10 mM glucose. As expected, g_i increases more slowly than g_e at all locations since diffusion takes place only in the interstitial spaces. After one minute, only cells near the islet periphery have a glucose concentration g_i of more than 50% of the bath solution. Even after two minutes, only those cells within about $20 \mu\text{m}$ of the islet

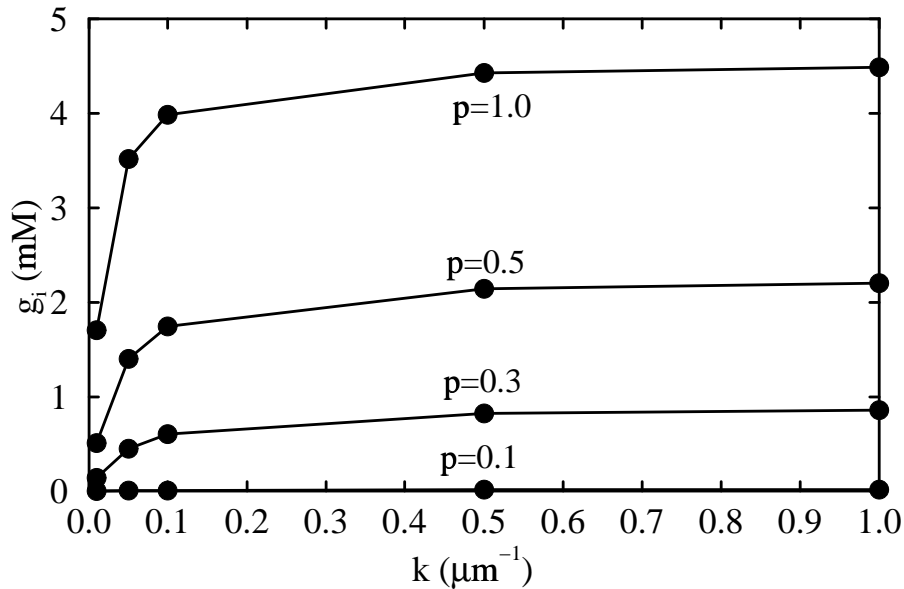


FIG. 5. β -cell glucose concentration at the location $r = 2 \mu\text{m}$ (near the islet center) two minutes after the simulated bath application of 10 mM glucose ($G = 10 \text{ mM}$).

periphery have achieved more than 50% of the bath glucose concentration. Hence, with the porosity and permeability values used here ($p = 0.3$ and $k = 0.3 \mu\text{m}^{-1}$), the glucose distribution in the islet is far from its equilibrium value of 10 mM two minutes after the introduction of glucose to the bath.

To analyze the effects of islet porosity and acinar layer permeability we focus on the β -cell glucose concentration at two extreme locations: the islet center and the islet periphery. Since islet electrical activity usually begins within about two minutes of the bath application of glucose, we examine the model β -cell glucose concentration at this point in time.

The β -cell glucose concentration at the islet center two minutes after the simulated bath application of 10 mM glucose is shown in Fig. 5. When the porosity is low, $p = 0.1$, almost no glucose reaches the islet center. Even when $p = 1$, so that the diffusion coefficient is that of glucose in water, g_i is less than 50% that of the perfusion solution. However, increasing the porosity from 0.1 to 1.0 does greatly increase g_i at the islet center. This is true for all values of the permeability coefficient. In contrast, although increasing the permeability from $k = 0.01$ to $1.0 \mu\text{m}^{-1}$ increases g_i at the islet center, the effect saturates when $k > 0.1 \mu\text{m}^{-1}$. These observations are consistent with results obtained in the absence of GLUT-2 transport (Fig. 3).

The glucose concentration at the islet periphery is much greater than that at the cen-

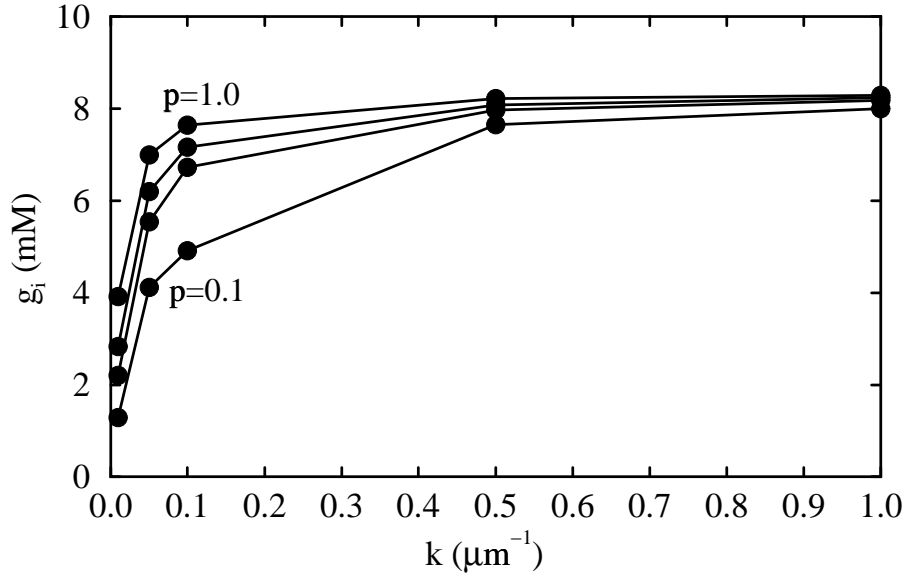


FIG. 6. β -cell glucose concentration at the location $r = 100 \mu\text{m}$ (the islet periphery) two minutes after the simulated bath application of 10 mM glucose. The porosity values for the four curves are (from top to bottom) $p = 1.0, 0.5, 0.3, 0.1$.

ter (Fig. 6). For most values of the porosity and permeability parameters g_i is more than 50% that of the bath, and g_i is close to 80% that of the bath when $k = 1 \mu\text{m}^{-1}$. As at the islet center, g_i at the periphery is greatly influenced by the islet porosity. Unlike g_i at the islet center, this influence begins to saturate when the permeability $k \geq 0.5 \mu\text{m}^{-1}$. For these values of p and k glucose transport into the peripheral β -cells is the rate limiting step to increases in g_i . As before, the effect of increasing acinar layer permeability begins to saturate when $k > 0.1 \mu\text{m}^{-1}$, although when porosity is low ($p = 0.1$) saturation occurs at a larger value of k .

Comparison With Autofluorescence Data

Two-photon excitation microscopy has recently been used to measure NAD(P)H autofluorescence in intact pancreatic islets (Bennett et al., 1996). Since NAD(P)H is a product of glucose metabolism, these measurements provide an indication of the glucose concentration within the islet cells. Using this approach, Bennett et al. were able to measure glucose penetration into an islet at several times following bath application of 30 mM glucose. In this section, we compare this NAD(P)H autofluorescence data to model simulations.

In Bennett et al. the NAD(P)H autofluorescence was measured in an optical section $40 \mu\text{m}$ into an isolated rat islet. At this depth, the diameter of the islet cross section was

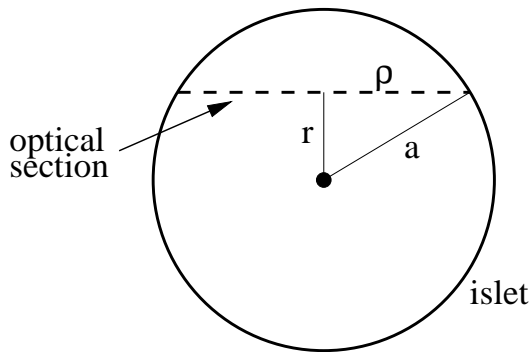


FIG. 7. Relation between the radius of an islet optical cross section (ρ), the islet radius (a), and the distance from the center of the cross section to the islet center (r).

approximately $110 \mu\text{m}$ (Fig. 3 of Bennett et al.). From this information, the islet radius can be determined. In Fig. 7 the islet is represented as a circle, and the optical section as a dashed line segment through the circle. The variables r , a , and ρ are related by the Pythagorean Theorem,

$$(20) \quad a^2 = r^2 + \rho^2 \quad .$$

The variable ρ is half the diameter of the islet cross section, so $\rho = 55 \mu\text{m}$. Since the optical section was taken at a depth of $40 \mu\text{m}$, $r = a - 40$. Substituting into Eq. 20 gives $a \approx 60 \mu\text{m}$. Therefore, the center of the islet cross section in Fig. 3 of Bennett et al. is approximately $20 \mu\text{m}$ from the center of an islet of radius $a = 60 \mu\text{m}$. This figure shows that NAD(P)H autofluorescence at the center of the section lags autofluorescence at the periphery by about 40 sec (presumably reflecting the glucose diffusion time). The K_m for the β -cell glucose sensor glucokinase is 5–10 μM (Johnson et al., 1990), so the intracellular glucose concentration at the center of the optical section should be in this range after 40 sec to account for the NAD(P)H production. Is the mathematical model consistent with this data?

Simulations were performed using the full model (using $p=0.3$, $k=0.3 \mu\text{m}^{-1}$). An islet radius of $60 \mu\text{m}$ was assumed, with $G = 30 \mu\text{M}$ and an initial (basal) glucose concentration of $1 \mu\text{M}$ for both g_i and g_e , consistent with the data. Forty seconds following the simulated application of glucose, it was found that the intracellular glucose concentration $20 \mu\text{m}$ from the islet center (corresponding to the center of the optical cross section) was $5.15 \mu\text{M}$ ($g_i(20, 40) = 5.15 \text{ mM}$). Although there may be significant NAD(P)H production at this glucose concentration, we next investigated the modifications in parameter values necessary to raise this to a higher level.

Although parameter values for the volume fraction ρ and the maximum glucose trans-

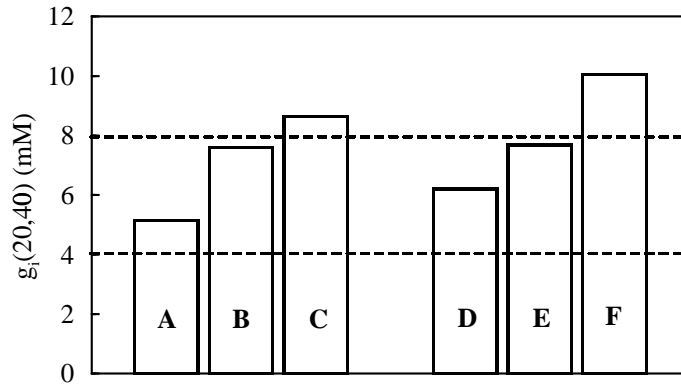


FIG. 8. The effects of changes in the parameters ρ , V_{max} , and D_i on the intracellular glucose concentration at the center of a hypothetical optical cross section 40 seconds after simulated bath application of 30 mM glucose. The optical section is 40 μm into an islet of radius 60 μm . In (D, E, F) intracellular diffusion is included, with $D_i = 6.73 \text{ cm}^2\text{sec}^{-1}$. (A, D) $\rho = 0.02$, $V_{max} = 0.53 \text{ mMsec}^{-1}$ (standard values); (B, E) $\rho = 0.04$, $V_{max} = 0.53 \text{ mMsec}^{-1}$; (C, F) $\rho = 0.04$, $V_{max} = 1.06 \text{ mMsec}^{-1}$. Other parameter values are $p = 0.3$, $k = 0.3$, and the initial (basal) glucose concentration is $g_i(r, 0) = g_e(r, 0) = 1 \text{ mM}$. The K_m for glucokinase is 5–10 mM, as indicated by the dashed lines.

port rate V_{max} were obtained from experimental data, it is likely that they vary from islet-to-islet. We therefore repeated the simulation described above with ρ doubled, and then with both ρ and V_{max} doubled. As shown in Fig. 8 (A, B, C), both changes in parameter values produced an increase in $g_i(20, 40)$, to values of 7.6 mM and 8.65 mM, respectively. The level of NAD(P)H production at either glucose concentration should be sufficient to account for the autofluorescence data.

The increased rate of glucose penetration resulting from a doubling of ρ is not surprising, since increasing ρ reduces the barrier to glucose diffusion. The effects of doubling V_{max} are not so clear. On the one hand, increasing V_{max} increases the flux of glucose into the β -cells, and since the NAD(P)H data reflects intracellular glucose an increase in g_i is to be expected. On the other hand, glucose transporters severely inhibit glucose penetration by transporting glucose from the interstitial spaces, where it can diffuse, to the β -cells, where it cannot diffuse. Thus, increasing V_{max} may be expected to decrease the rate of glucose penetration. Because of these competing influences, the effects of changes in V_{max} are hard to predict. In fact, although doubling V_{max} increases $g_i(20, 40)$ when $\rho = 0.4$, doubling V_{max} decreases $g_i(20, 40)$ when $\rho = 0.2$ (not shown).

One assumption made in of our model is that glucose diffuses only through interstitial spaces. However, there is data showing that glucose can diffuse through gap junctions (Rieske et al., 1975). If this is the case in pancreatic islets, then it is likely that the process is quite complex. We have incorporated intracellular diffusion into the model in a very

simplistic fashion by adding a diffusion term to Eq. 5, yielding:

$$(21) \quad \frac{\partial g_i}{\partial t} = \frac{D_i}{r^2} \frac{\partial}{\partial r} \left(r^2 \frac{\partial g_i}{\partial r} \right) + F(g_e, g_i) \quad ,$$

with the accompanying boundary condition:

$$(22) \quad \frac{\partial g_i}{\partial r} = 0 \quad , \quad r = a \quad ,$$

assuming that glucose does not enter the β -cells directly from the external solution, but must be transported from the interstitial solution.

It is highly likely that the glucose diffusion rate through gap junctions is much lower than the diffusion rate in water (D), so we have used $D_i = D/100 = 6.73 \text{ cm}^2\text{sec}^{-1}$ in the simulations reported in (**D**, **E**, **F**) of Fig. 8. Except for the addition of intracellular diffusion, these simulations are identical to (**A**, **B**, **C**). It is evident that intracellular diffusion increases the rate of glucose penetration into the islet for each parameter combination. Furthermore, the impact of intracellular diffusion is greater for larger values of the glucose transport rate V_{max} .

Even if glucose diffusion through gap junctions is insignificant, there are other means for intracellular diffusion to occur. For example, glucose could enter a β -cell through GLUT-2 transporters on one face of the cell and leave through similar transporters on the other face. Like diffusion through gap junctions, this is a complex process, but Eq. 21 provides a reasonable first approximation.

DISCUSSION

The aim of this study was to determine the glucose distribution in a typical pancreatic islet shortly after the addition of a stimulatory concentration of glucose to the bath. Given the assumptions made in the model, we found that the glucose distribution in an islet of radius $100 \mu\text{m}$ was far from uniform two minutes after the bath application of 10 mM glucose. The glucose concentration within β -cells was less than 5 mM at the islet center and greater than 5 mM only near the islet periphery for a range of values of islet porosity and acinar layer permeability (Figs. 4–6). Isolated β -cells typically become electrically active when exposed to glucose concentrations of 7 mM or more (Atwater et al., 1984). Thus, our analysis suggests that, with this glucose application protocol, only the cells near the islet periphery are exposed to a stimulatory concentration of glucose within two minutes of glucose application. This two minute period is significant since β -cell electrical activity typically begins within two minutes of the bath application of glucose.

There is a large body of evidence that the electrical activity of β -cells within an islet is synchronized, due at least in part to gap-junctional coupling (Eddlestone et al., 1984; Santos et al., 1991). Our modeling results indicate that the electrical activity begins before the intra-islet glucose concentration has equilibrated. Thus, it appears that islets are capable of synchronized electrical activity even though only the peripheral cells are exposed to stimulatory glucose concentrations. This complements earlier modeling studies showing that clusters of model β -cells are capable of generating bursts of electrical impulses even though the majority of cells in the cluster contain subthreshold glucose concentrations (Pernarowski, 1997; Smolen et al., 1993).

We examined the effects of islet porosity and acinar layer permeability on glucose penetration (Figs. 3, 5, 6 and Eqs. 17, 18). It was shown that both can have a dramatic impact, and that the efficacy of one parameter depends largely on the value of the other, as well as the location in the islet. There is little experimental data for the values of these parameters, and it is likely that they vary greatly from islet to islet.

The transport of glucose into β -cells by GLUT-2 transporters profoundly slows glucose penetration into the islet. Using the maximum value for islet porosity ($p = 1$) and a saturating value for acinar layer permeability ($k = 1 \mu\text{m}^{-1}$) it was shown that the interstitial glucose concentration g_e at the islet center reaches 90% of the bath concentration in only a few seconds in the absence of glucose transport (Fig. 3). When transport does occur, it takes five minutes to reach this 90% point. Thus, GLUT-2 transport provides β -cells with glucose at the expense of slowing glucose delivery to cells in the islet interior. This may help explain why substrates such as carbachol and tolbutamide, which have a molecular weight near that of glucose but are not actively transported into β -cells, act much more quickly than does glucose (Bozem and Henquin, 1988; Gilon and Henquin, 1992). That is, because carbachol and tolbutamide can diffuse through the islet without being transported into β -cells, Fig. 3 suggests that equilibration can occur in a few seconds.

In this report, we compared glucose penetration times predicted by the model with recent NAD(P)H autofluorescence data (Bennett et al., 1996). We found that the model is able to account for the data, particularly if the volume fraction ρ and the maximum GLUT-2 transport rate V_{max} are appropriately modified (Fig. 8), which seems reasonable given the great islet-to-islet and cell-to-cell variability. The rate of penetration of glucose into the islet is also significantly increased if some intracellular diffusion occurs (Fig. 8). Indeed, glucose diffusion through gap junctions has been reported in leech central nervous neurons (Rieske et al., 1975). There may be additional means for intracellular diffusion. For example, glucose could enter a β -cell through GLUT-2 transporters at one face and

leave through similar transporters at the opposite face. By adding a diffusion term to the g_i equation (Eq. 21), we provide a reasonable first approximation to either mechanism of intracellular diffusion. However, more detailed modeling of these processes could lead to new insights, and should be performed in the future.

One may question whether the permeability and porosity values used in our comparison simulations ($p = 0.3$, $k = 0.3$) are unrealistically high. Due to a lack of data, this question cannot be answered at present, although we note that the effective diffusion coefficient of K^+ in an islet was measured to be about half of its value in water (Perez-Armendariz et al., 1985). If indeed the permeability and porosity values are unrealistically high, then this suggests that some factor in addition to diffusion is responsible for glucose penetration into the islet.

The one to two minute delay in islet electrical activity typically observed following bath application of glucose is due in large part to the time required for glucose metabolism and the subsequent inactivation of $K(ATP)$ channels in the β -cells. However, the relatively long time required for glucose to diffuse from the islet periphery to the interior (Fig. 4–6) suggests that glucose diffusion may also be a major contributing factor. Experimental support for the role of diffusion in the delay in electrical activity is provided by several studies of isolated β -cells. In one study, bath application of glucose produced an almost immediate increase in the ratio of ATP to ADP, indicating that little time is required for the metabolism of glucose by β -cells (Nilsson et al., 1996). In two other studies, bath application of glucose elicited electrical activity or an elevation in cytosolic Ca^{2+} with a delay of less than 20 seconds (Liu et al., 1994; Larsson et al., 1996), suggesting that less than 20 seconds is required for β -cells to metabolize glucose and inhibit ATP-sensitive K^+ channels. We point out, however, that in one study the delay in spiking activity following a step increase in the bath glucose concentration was nearly one minute (Chow et al., 1995). In another study, inhibition of $K(ATP)$ channel activity was delayed by nearly two minutes (Valdeolmillos et al., 1992). However, the channel activity was measured at room temperature, where one would expect exaggerated delays. The bulk of these single cell studies suggest that although intracellular delays in glucose handling are a major factor in the delay in islet electrical activity, there is likely a second contributing factor. Our analysis supports the hypothesis that this additional factor is the time required for glucose to diffuse through the islet.

One common observation is that the delay in electrical activity depends on the extent of previous exposure to glucose. Thus, a recent history of exposure to low glucose will result in an exaggerated delay in electrical activity. This can be explained in at least two

ways. First, following a prolonged low level of ATP, glucose metabolism and K(ATP) channel inactivation in β -cells may be slowed. Second, the time required for islet cells to achieve a threshold glucose concentration will be greater since the initial distribution is lower. This latter effect is consistent with model simulations (not shown).

The mathematical model used in the present study is based on several assumptions and simplifications that seem justified given the lack of data to support a more detailed model and given the great islet-to-islet variability. The acinar layer was assumed to act as a passive membrane, allowing only the diffusive transport of glucose into the islet. At higher perfusion flow rates this assumption could lead to inaccuracies. Furthermore, at high membrane permeabilities convective transport of glucose through the islet would play a more important role.

It was also assumed that the glucose concentration can be treated as a continuous variable both within and outside of the β -cells. This assumption justifies the simplified definition for effective diffusivity of glucose within the islet. In other systems, attempts have been made to more accurately model the effect of cell packing, geometry and heterogeneity on effective diffusivity through the use of multiphase averaging techniques (Ochoa et al., 1986). However, implementation of these techniques in the pancreatic islet appears to be impractical since the required *a priori* knowledge of islet morphology and heterogeneity is not available.

Spherical symmetry in the distribution of glucose follows from the spherical shape of the islet and from the assumption of uniform β -cell distribution and a uniform density of GLUT-2 transporters within β -cells. In most of the analysis it was also assumed that glucose does not diffuse through gap junctions, although this assumption was relaxed later. Lastly, most of the simulations presented had an initial glucose concentration of zero in the islet. This was done primarily for convenience. As was alluded to above, an initial concentration of 2 or 3 mM may be more appropriate for many experimental protocols (or perhaps higher for islets with a prior history of exposure to high glucose). Though, as was previously noted, in the absence of GLUT-2 transport only the initial difference in islet and bath concentrations affect the characteristic diffusion time.

In summary, this study suggests that glucose equilibration in a previously glucose-free isolated islet takes at least five minutes. This suggests that synchronized electrical activity begins long before glucose equilibration. The dominant factor in the delay in glucose penetration is the transport of glucose into β -cells by GLUT-2 transporters. The delay in glucose penetration is likely a major contributing factor in the one to two minute delay in electrical activity following glucose application.

APPENDIX

I. Series Solution of Equations Without Transport

Here we present the derivation of the series solution of Eqs. 7-10 via the method of separation of variables. Substituting $c(r, t) = R(r)T(t)$ into Eq. 7 we obtain

$$(23) \quad \frac{T'}{pDT} = \frac{r^2 R'' + 2r R'}{r^2 R} = -\lambda^2$$

where λ is a constant due to the dependence of T and R on the different independent variables t and r , respectively. The boundary conditions Eqs. 8-9 yield the following eigenvalue problem for $R(r)$:

$$(24) \quad r^2 R'' + 2r R' + \lambda^2 r^2 R = 0 \quad , \quad r < a \quad ,$$

$$(25) \quad R'(a) + kR(a) = 0 \quad ,$$

$$(26) \quad |R| \leq M < \infty \quad .$$

The solution of Eq. 24 for $\lambda > 0$ is given in terms of Bessel functions of order 1/2. Since only the Bessel function of the first kind is bounded near 0, the solutions $R(r)$ satisfying Eq. 26 are

$$(27) \quad R_\lambda(r) = \sqrt{\frac{\pi}{2r}} J_{1/2}(\lambda r) = \frac{\sin(\lambda r)}{\sqrt{\lambda r}} \quad .$$

An eigenvalue equation for λ is then obtained by requiring $R_\lambda(r)$ to satisfy the boundary condition Eq. 25:

$$(28) \quad (ka - 1) \tan \mu + \mu = 0 \quad , \quad \mu = \lambda a \quad .$$

Providing $ka \neq 1$, Eq. 28 has a countable number of solutions $0 < \lambda_1 < \lambda_2 < \dots$, generating the corresponding eigenfunctions

$$(29) \quad R_n(r) = \frac{\sin(\lambda_n r)}{\sqrt{\lambda_n r}} \quad .$$

The function $T(t)$ satisfies the differential equation

$$(30) \quad T' = -\lambda^2 pDT \quad , \quad t > 0$$

with solution $T(t) = \exp(-\lambda^2 pDt) = \exp(-\lambda_n^2 pDt)$ for $\lambda = \lambda_n$. Therefore, the series solution for $c(r, t)$ assumes the form

$$(31) \quad c(r, t) = \sum_{n=1}^{\infty} \hat{a}_n \exp(-\lambda_n^2 pDt) R_n(r) \quad .$$

The solution is completed using the known initial condition $c(r, 0) = G - g_e(r, 0)$ and the orthogonality of $R_n(r)$ under the inner product

$$(32) \quad \langle \phi, \psi \rangle \equiv \int_0^a \phi(r)\psi(r)w(r)dr = \int_0^a \phi(r)\psi(r)r^2 dr$$

with the weight function $w(r) = r^2$ for the Laplacian operator in spherical coordinates. These calculations yield

$$(33) \quad \hat{a}_n = \frac{\langle c(r, 0), R_n(r) \rangle}{\langle R_n(r), R_n(r) \rangle} \quad ,$$

and for the special case $c(r, 0) = G$,

$$(34) \quad \hat{a}_n = Ga_n = \frac{4G(\sin(\lambda_n a) - a\lambda_n \cos(\lambda_n a))}{\sqrt{\lambda_n}(2\lambda_n a - \sin(2\lambda_n a))} \quad .$$

It should be noted that the convergence of the series solution in Eq. 31 is in the mean and need not be pointwise. In particular, one should not expect pointwise convergence at $r = 0$ at which the series is formally undefined.

II. Table of Parameter Values

Symbol	Description	Value	Reference
D	glucose diffusivity in water	0.673×10^{-5} cm ² /sec	Weast, 1975
a	islet radius	100 μ m	Atwater et al., 1989
ρ	volume fraction	0.02	Bonner-Weir, 1988
K_m	GLUT-2 dissociation constant	17 mM	Johnson et al., 1990
V_{max}	GLUT-2 max. uptake rate	0.53 mM/sec	Johnson et al., 1990
k	acinar layer permeability	0.02 – 1.0 μ m ⁻¹	
p	islet porosity	0.02 – 1	

We thank anonymous reviewers for constructive comments that led to improvements in the manuscript. M.P. was supported by the National Science Foundation grants OSR-93-50-546 and DMS-97-04-966.

REFERENCES

- [1] F. M. Ashcroft, D. E. Harrison, and S. J. H. Ashcroft. Glucose induces closure of single potassium channels in isolated rat pancreatic β -cells. *Nature*, 312:446–448, 1984.
- [2] I. Atwater, P. Carroll, and M. X. Li. Electrophysiology of the pancreatic β -cell. In B. Drazin, S. Melmed, and D. LeRoith, editors, *Insulin Secretion*, pages 49–68. Alan R. Liss, Inc., New York, 1989.
- [3] I. Atwater, A. Gonçalves, A. Herchuelz, P. Lebrun, W. J. Malaisse, E. Rojas, and A. Scott. Cooling dissociates glucose-induced release from electrical activity and cation fluxes in rodent pancreatic islets. *J. Physiol. (Lond.)*, 348:615–627, 1984.
- [4] B. D. Bennett, T. L. Jetton, G. Ying, M. A. Magnuson, and D. W. Piston. Quantitative subcellular imaging of glucose metabolism within intact pancreatic islets. *J. Biol. Chem.*, 271:3647–3651, 1996.
- [5] S. Bonner-Weir. Morphological evidence for pancreatic polarity of β -cells within islets of Langerhans. *Diabetes*, 37:616–621, 1988.
- [6] M. Bozem and J. -C. Henquin. Glucose modulation of spike activity independently from changes in slow waves of membrane potential in mouse β -cells. *Pflügers Arch.*, 413:147–152, 1988.
- [7] R. H. Chow, P.-E. Lund, S. Löser, U. Panten, and E. Gylfe. Coincidence of early glucose-induced depolarization with lowering of cytoplasmic Ca^{2+} in mouse pancreatic β -cells. *J. Physiol. (Lond.)*, 485:607–617, 1995.
- [8] D. L. Cook and E. Perara. Islet electrical pacemaker response to alpha-adrenergic stimulation. *Diabetes*, 31:985–990, 1982.
- [9] P. M. Dean and E. K. Mathews. Glucose-induced electrical activity in pancreatic islet cells. *J. Physiol. (Lond.)*, 210:255–264, 1970.
- [10] E. J. Doedel. Auto: A program for the automatic bifurcation and analysis of autonomous systems. *Proc. 10th Manitoba Conf. on Numer. Math. and Comput. Winnipeg, Canada*, 30:265–284, 1981.
- [11] G. T. Eddlestone, A. Gonçalves, J. A. Bangham, and E. Rojas. Electrical coupling between cells in islets of Langerhans from mouse. *J. Membr. Biol.*, 77:1–14, 1984.
- [12] B. Ermentrout. XTC—A tool for modeling spatial evolution equations (bardmthbard.math.pitt.edu). 1995.
- [13] P. Gilon and J. -C. Henquin. Influence of membrane potential changes on cytoplasmic Ca^{2+} concentration in an electrically excitable cell, the insulin-secreting pancreatic β -cell. *J. Biol. Chem.*, 267:20713–20720, 1992.
- [14] H. Heimberg, A. De Vos, D. Pipeleers, B. Thorens, and F. Schuit. Differences in glucose transporter gene expression between rat pancreatic α - and β -cells are correlated to differences in glucose transport but not in glucose utilization. *J. Biol. Chem.*, 270:8971–8975, 1995.
- [15] J. -C. Henquin, M. -C. Garcia, M. Bozem, M. P. Herman, and M. Nenquin. Muscarinic control of pancreatic B cell function involves sodium-dependent depolarization and calcium influx. *Endocrinology*, 122:2134–2142, 1988.
- [16] J. H. Johnson, C. B. Newgard, J. L. Milburn, H. F. Lodish, and B. Thorens. The high K_m glucose transporter of islets of Langerhans is functionally similar to the low affinity transporter of liver and has an identical primary sequence. *J. Biol. Chem.*, 265:6548–6551, 1990.
- [17] O. Larsson, H. Kindmark, R. Bräanström, B. Fredholm, and P.-O. Berggren. Oscillations in K_{ATP} channel activity promote oscillations in cytoplasmic free Ca^{2+} concentration in the pancreatic

- β -cell. *Proc. Natl. Acad. Sci. USA*, 93:5161–5165, 1996.
- [18] Y. J. Liu, E. Grapengiesser, E. Gylfe, and B. Hellman. Glucose-induced oscillations of Ba^{2+} in pancreatic β -cells occur without involvement of intracellular mobilization. *Arch. Biochem. Biophys.*, 315(2):387–392, 1994.
- [19] L. W. Maki and J. Keizer. Analysis of possible mechanisms for in vitro oscillations of insulin secretion. *Am. J. Physiol.*, 268:C780–C791, 1995.
- [20] D. Mears. *Biophysical properties and functional roles of ionic currents in the pancreatic beta cell*. PhD thesis, Johns Hopkins University, Baltimore, MD, 1996.
- [21] T. Nilsson, V. Schultz, P.-O. Berggren, B. E. Corkey, and K. Tornheim. Temporal patterns of changes in ATP/ADP ratio, glucose 6-phosphate and cytoplasmic free Ca^{2+} in glucose-stimulated pancreatic β -cells. *Biochem. J.*, 314:91–94, 1996.
- [22] J. A. Ochoa, P. Stroeve, and S. Whitaker. Diffusion and reaction in cellular media. *Chem. Eng. Science*, 41:2999–3013, 1986.
- [23] E. Perez-Armendariz, I. Atwater, and E. Rojas. Glucose-induced oscillatory changes in extracellular ionized potassium concentration in mouse islets of langerhans. *Biophys. J.*, 48:741–749, 1985.
- [24] M. Pernarowski. Fast and slow subsystems for a continuum model of bursting activity in the pancreatic islet. *SIAM J. Appl. Math.*, in press.
- [25] E. Rieske, P. Schubert, and G.M. Kreutzberg. Transfer of radioactive material between electrically coupled neurons of the leech central nervous system. *Brain Res.*, 84:365–382, 1975.
- [26] J. V. Sánchez-Andrés, A. Gomis, and M. Valdeolmillos. The electrical activity of mouse pancreatic β -cells recorded *in vivo* shows glucose-dependent oscillations. *J. Physiol. (Lond.)*, 486:223–228, 1995.
- [27] R. M. Santos, L. M. Rosario, A. Nadal, J. Garcia-Sancho, B. Soria, and M. Valdeolmillos. Widespread synchronous $[Ca^{2+}]_i$ oscillations due to bursting electrical activity in single pancreatic islets. *Pflügers Arch.*, 418:417–422, 1991.
- [28] A. M. Scott, I. Atwater, and E. Rojas. A method for the simultaneous measurement of insulin release and B cell membrane potential in single mouse islets of Langerhans. *Diabetologia*, 21:470–475, 1981.
- [29] P. A. Smith, F. M. Ashcroft, and P. Rorsman. Simultaneous recordings of glucose dependent electrical activity and ATP-regulated K^+ -currents in isolated mouse pancreatic β -cells. *FEBS Lett.*, 261:187–190, 1990.
- [30] P. Smolen, J. Rinzel, and A. Sherman. Why pancreatic islets burst but single β -cells do not: the heterogeneity hypothesis. *Biophys. J.*, 64:1668–1679, 1993.
- [31] B. Soria, F. Martín, E. Andreu, J. V. Sanchez-Andrés, V. Nacher, and E. Montana. Diminished fraction of blockable ATP-sensitive K^+ channels in islets transplanted into diabetic mice. *Diabetes*, 45:1755–1760, 1996.
- [32] R. H. Unger. Diabetic hyperglycemia: Link to impaired glucose transport in pancreatic β cells. *Science*, 251:1200–1205, 1991.
- [33] M. Valdeolmillos, A. Nadal, D. Contreras, and B. Soria. The relationship between glucose-induced K_{ATP} channel closure and the rise in $[Ca^{2+}]_i$ in single mouse pancreatic β -cells. *J. Physiol. (Lond.)*, 455:173–186, 1992.
- [34] R. C. Weast. *Handbook of Chemistry and Physics*. CRC Press, Cleveland, Ohio, 1975.
- [35] R. R. Whitesell, A. C. Powers, D. M. Regen, and N. A. Abumrad. Transport and metabolism of glucose in an insulin-secreting cell line, β TC-1. *Biochemistry*, 30:11560–11566, 1991.

- [36] J. F. Worley III, M. S. McIntyre, B. Spencer, R. J. Mertz, M. W. Roe, and I. D. Dukes. Endoplasmic reticulum calcium store regulates membrane potential in mouse islet β -cells. *J. Biol. Chem.*, 269:14359–14362, 1994.